Modelling Cable Vibration Following Load Removal

Mouna Ammar and László E. Kollár(✉)

Savaria Institute of Technology, ELTE Eötvös Loránd University, Károlyi G. tér 4, 9700 Budapest, Szombathely, Hungary
kl@inf.elte.hu

Abstract. Cable vibration due to different load removal scenarios is modelled numerically and experimentally. The numerical model considers a conductor in one span of a transmission line, which is loaded by ice. The experimental set-up represents a small-scale model of the transmission line with ice-loaded conductor. Load removal simulates ice shedding that leads to conductor jump followed by a decaying vibration. Dynamic effects of partial ice shedding from different parts of the conductor are compared. The study reveals the increasing tendency in the maximum value of the vertical displacement and the tension in the conductor during vibration with the increasing amount of shedding load. The practical benefit from the prediction of these parameters is that they help assess to what extent the clearance reduces between vibrating conductors and what dynamic forces act in the conductor during vibration.

Keywords: Cable vibration · Experiment · Load removal · Modelling

1 Introduction

Overhead transmission lines are subjected to multiple types of external load due to ice or wind, which cause high mechanical stresses and vibration of the conductors. Such vibration may be caused by wind load, but it may also be the result of ice shedding. This phenomenon is associated with high conductor rebound height and great transient dynamic forces, which motivated the research effort to study the background and model the phenomenon by load removal tests. The first experimental and numerical models have been published several decades ago [1, 2]. The dynamic effects of ice shedding on conductor bundles were simulated numerically and in laboratory tests considering sudden shedding [3] and ice shedding propagation [4]. Reference [5] suggested a formula based on numerical simulations, whereas Reference [6] developed a theoretical method to calculate conductor rebound height following ice shedding. Previously developed formulae were evaluated and modified in [7]. Reference [8] proposed a theoretical model that simulates ice-shedding-induced conductor vibration at a specific position where an active control is applied to attenuate the vibration. The present research developed an experimental and a numerical model to simulate ice shedding from conductors, which are applicable to predict conductor tension and rebound height during vibration, and discusses the effects of shedding from partially loaded conductors.

M. Okada (Ed.): IFToMM WC 2023, MMS 149, pp. 891–900, 2024.
https://doi.org/10.1007/978-3-031-45709-8_87

2 Experimental Model of Reduced-Scale Transmission Line

2.1 Experimental Set-Up

The experimental model consists of a reduced-scale span of a transmission line, which is set up in the laboratory of the Savaria Institute of Technology at ELTE Eötvös Loránd University, Budapest. The experimental set-up is sketched in Fig. 1. The T7x19 stainless steel cable with diameter of 4 mm is suspended between two supports resulting in a span length of 16.624 m and a sag of 0.305 m.

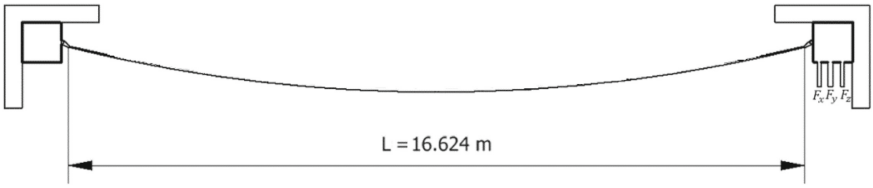

Fig. 1. Sketch of the reduced scale model of a single span conductor

The suspended cable is attached to an HBM MCS10–005-3C-FX-FY-FZ-00–00-00 load cell at one of the fixed supports as shown in Fig. 2a. The load cell measures the 3 components of the force reactions. It is connected to an HBM QuantumX MX840B data acquisition module that collects the data measured and transfers them to a computer where results are visualized using the HBM CatmanEasy AP software.

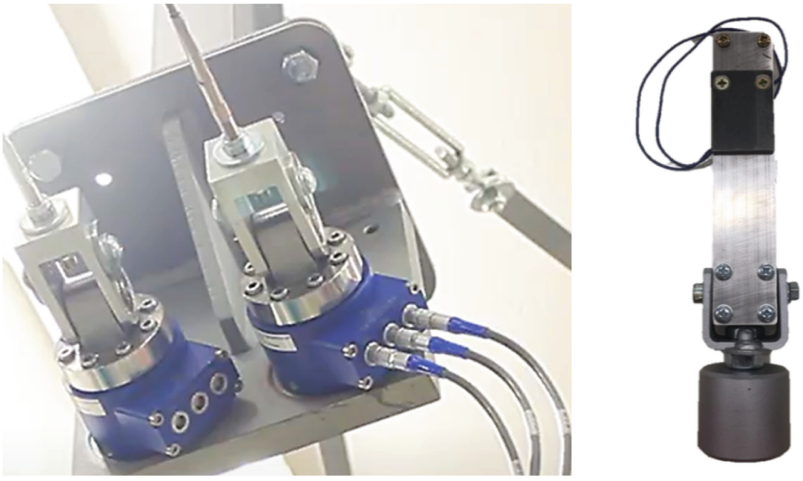

(a) (b)

Fig. 2. Equipment for experiments; (a) load cells at the support (only the conductor and the load cell on the right side were used in the experiments presented); (b) load unit with electromagnet

Ice occurs as a distributed load on the conductor, which is modelled by several concentrated loads (see Fig. 2b). Since uniform ice load is assumed, the concentrated

loads are identical, each of them having a mass of 0.8 kg. Loads are attached to the cable via electromagnets that are controlled by a microcontroller device [9]. Loads were also hinged to the roof via loose wires in order to prevent the loads from falling on the floor and causing damage. Altogether 17 loads may be attached to the cable, but their number depends on the location where ice is assumed. Ice shedding is simulated by the removal of the loads at specified time instances. Commands can be programmed in the microcontroller, and they determine time instances when an electromagnet should be switched on or off. The electromagnets on the loads are switched on when the loads are attached, and the time instance when they are switched off is programmed.

Sudden ice shedding is simulated, correspondingly the electromagnets on all the attached loads are switched off at the same time instance. Controlling the magnets is achieved by sending data to the microcontroller via the serial monitor of the program Energia. The PuTTY software may also be used to apply the commands to the microcontroller. Details of the commands and their application to load removal are given in [9] and [10].

2.2 Measurement

The experimental set-up is designed to simulate load shedding with the resulting conductor vibration and to measure the maximum vertical displacement of the conductor together with the variation of the force at the suspension after load removal. The loads are attached on marked positions, with varying their number from 3 to 17 in consecutive tests as shown in Table 1. The measurements start when the loads are attached to the conductor so that the load cells provide the additional force acting in the cable due to the loads attached. After a while, when the loaded cable reached its new static equilibrium, the loads are detached as programmed in the microcontroller device and the vibration takes place as a response to the load shedding. The cable rebound height, i.e. its highest vertical displacement is measured by means of a scale-meter attached to a white background placed behind the experimental model of the span.

Table 1. Load shedding scenarios in the experimental tests

	Number of loads	Load location	Time variation
1	3	From 0.41L to 0.59L	All loads shed at the same time
2	7	From 0.29L to 0.71L	All loads shed at the same time
3	11	From 0.18L to 0.82L	All loads shed at the same time
4	17	All over the span	All loads shed at the same time

There are many possible scenarios for ice shedding. Some typical scenarios are simulated in the present project, when smaller or greater parts of the span is loaded or the entire span is loaded, and all the loads shed at the same time. These scenarios are summarized in Table 1.

3 Numerical Model of Cable Vibration Following Load Shedding

3.1 Aim of the Analysis

The numerical model of load shedding from the suspended conductor was constructed and the resulting vibration is carried out using the finite element analysis software Ansys. The vertical displacement of the conductor and the cable tension are calculated during the vibration, which provide the jump height of the conductor and the peak force acting at the suspension.

In the numerical model, the load on the cable can be considered in two different ways. First, point loads are applied, exactly like in the experiments, and then distributed load is applied on the loaded part of the cable. Reference [3] revealed that if a high enough number of point loads is applied along the loaded part of the cable, then the loaded position and the vibration following load removal closely approximates those obtained after the application and removal of distributed load.

3.2 Description of Geometrical and Material Model

The conductor is considered by a line body model in Ansys Workbench. The geometrical parameters of the cable and the span are listed in Table 2. The T7x19 stainless steel cable used in the experiments was defined in the numerical model as well. The material properties considered in the model are also given in Table 2.

Table 2. Geometrical and material properties of the conductor and span

Parameters	Symbol	Value
Span length (m)	L	16.62
Sag (m)	f	0.305
Mass per unit length (kg/m)	μ	0.061
Young's modulus (GPa)	E	60
Cross section area (mm^2)	A	7.5
Envelop diameter (mm)	D	4
Density (kg/m^3)	ρ	8133

3.3 Boundary Conditions

The conductor is hinged at both ends, and it is subjected to its own weight. In order to model its static profile, the earth gravitational acceleration is applied with a value of $g = 9.81$ m/s^2. Later on, an initial tension is defined as a pre-strain in the cable. Since the cable length is slightly longer than the span length, a remote displacement was applied at one end in order to reach the span length with the catenary profile obtained. Once these kinematic conditions are applied, the cable slightly swings until it reaches

the static equilibrium. Then the dynamic boundary conditions are considered by adding concentrated loads gradually on the edges marked in the cable, each of them with a value of $F = 7.848$ N. The magnitude of the force is based on the weight of loads that were used in the experiments. Then the loads shed from the conductor, followed by vibration. The model simulates the dynamic response of the conductor until it reaches the steady state in the unloaded equilibrium. The kinematic and dynamic boundary conditions are summarized in Table 3, and the locations of their application are illustrated in Fig. 3.

Table 3. Kinematic and dynamic boundary conditions

Kinematic boundary conditions	Dynamic boundary conditions
A—Fixed support: Fix the left end of the suspended cable	C—Standard earth gravity: Applied on the full structure with a standard value of $g = 9806.6$ mm/s^2
B—Remote displacement: Move the right end of the cable according to the span length and fix it	D—Force (point load): Simulate the weight of the load modelling ice, applied on 3, 7, 11 or 17 points depending on the load case

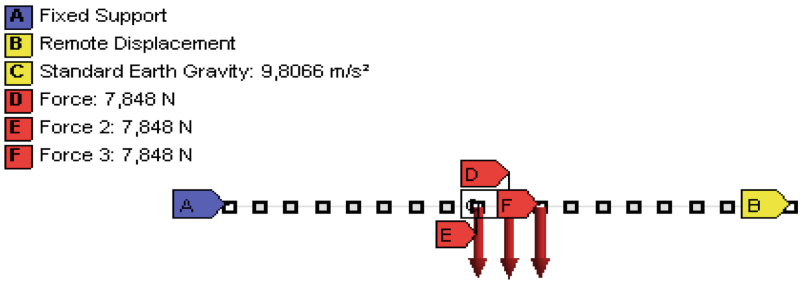

Fig. 3. Boundary conditions applied on the cable

Load removal is followed by high-amplitude vibration that then decays due to the structural damping of the conductor. This damping was considered by numerical damping in the model. Aerodynamic damping may also be important under some conditions, but it was not taken into account in the numerical model.

4 Results

Results of numerical simulations and experiments are presented in this section. First, the numerical model is validated by comparing the jump heights obtained numerically and experimentally, and then the time histories of vertical displacement and force reaction at the suspension are studied. Simulations and measurements are carried out for the load shedding scenarios discussed in Sect. 2.2, and time histories are shown for the case of 7 point loads.

4.1 Model Validation

The numerical and experimental results are compared in Fig. 4 in order to validate the numerical model. The maximum vertical displacements during the vibration following load removal are compared. The numerical model underestimates the cable jump obtained experimentally, but the error reduces to the range of 5% when the loaded part of the span is not very small. The similarity of the results suggests that the numerical model is reliable to describe the dynamics of the cable after load removal.

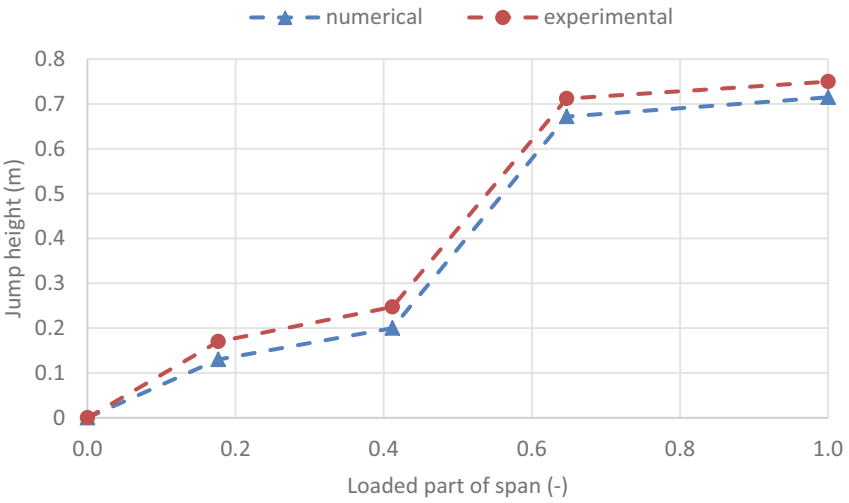

Fig. 4. Comparison of cable jump height obtained numerically and experimentally

4.2 Numerical Results

Vertical displacement. The time history of the vertical displacement of the cable at midspan after 7 point loads are removed is shown in Fig. 5. The sag in the static equilibrium is 0.305 m that is obtained after the remote displacement and standard earth gravity are applied (see $t = 19$ s). The point loads are added at $t = 20$ s, and the new static equilibrium in the loaded position is reached after a few seconds. The increased sag in this position is 0.40 m. Note that the oscillation in the displacement occurs, because transient structural model is applied, but the simulation of the physical process of load shedding begins only at $t = 25$ s. The highest position of the cable during the vibration is 0.20 m below the zero vertical position, i.e. below the height of the suspension points, which means a jump height of 0.20 m above the loaded position. Figure 5 also confirms that the application and removal of point loads approximate closely the application and removal of distributed load in the same part of the cable. The jump heights above the loaded position for the other cases considered (i.e. after the removal of 3, 11 and 17 loads) are shown by the blue triangles in Fig. 4.

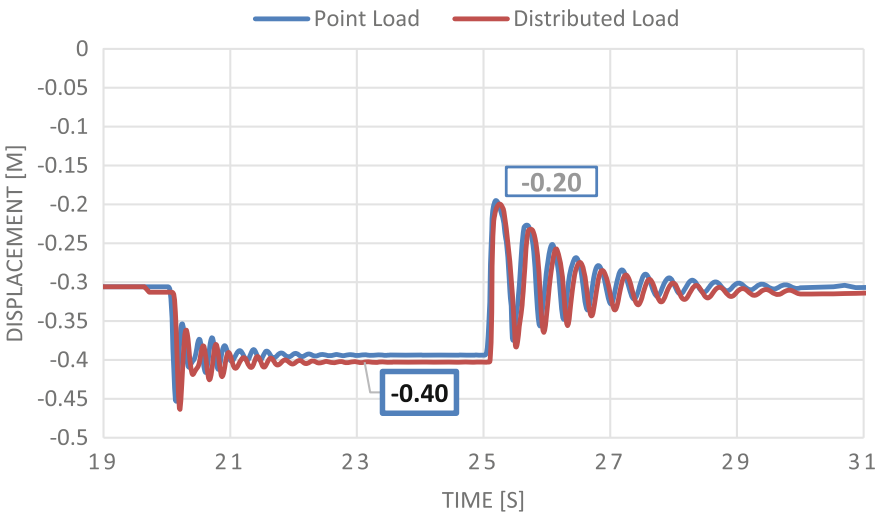

Fig. 5. Time history of vertical displacement of the cable at mid-span; the 7 point loads are added at $t = 20$ s, and they are removed at $t = 25$ s

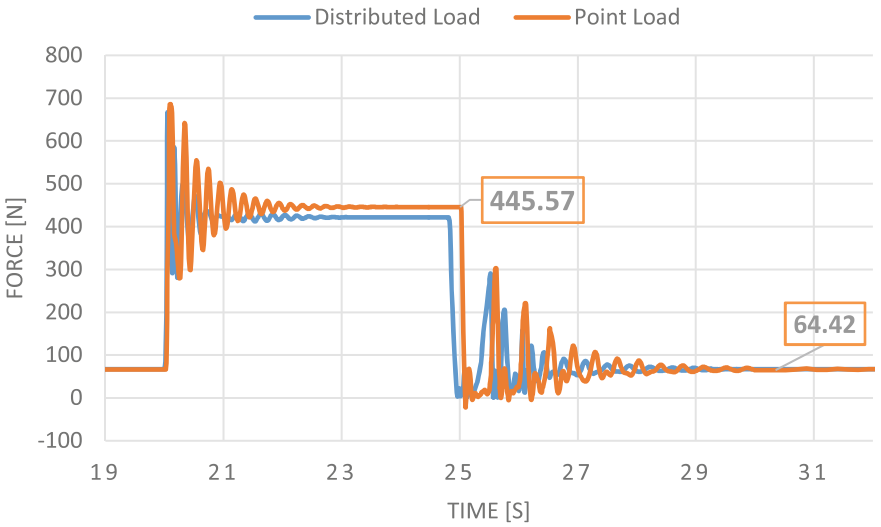

Fig. 6. Time history of force reaction in the numerical simulation; the 7 point loads are added at $t = 20$ s, and they are removed at $t = 25$ s

Force Reaction. The time history of force reaction as obtained in the numerical simulation after the application and removal of 7 point loads is plotted in Fig. 6. The force at the suspension when the cable is loaded is 445.6 N. The force oscillates after load removal, but it does not reach this value again during the vibration that decays. Finally, the force reaches the value of 64.4 N in the static equilibrium of the unloaded cable.

4.3 Experimental Results

The time history of force reaction as obtained in the experiments after the application and removal of 7 point loads is plotted in Fig. 7. The measurements with the microcontroller started at the moment when the loads were attached one by one, which was approximately at $t = 32$ s. The force at the suspension when the cable is loaded was obtained after a few seconds when the cable reached the equilibrium, and this value was 447 N. The loads were removed at $t = 35$ s, and similarly to the numerical simulation,

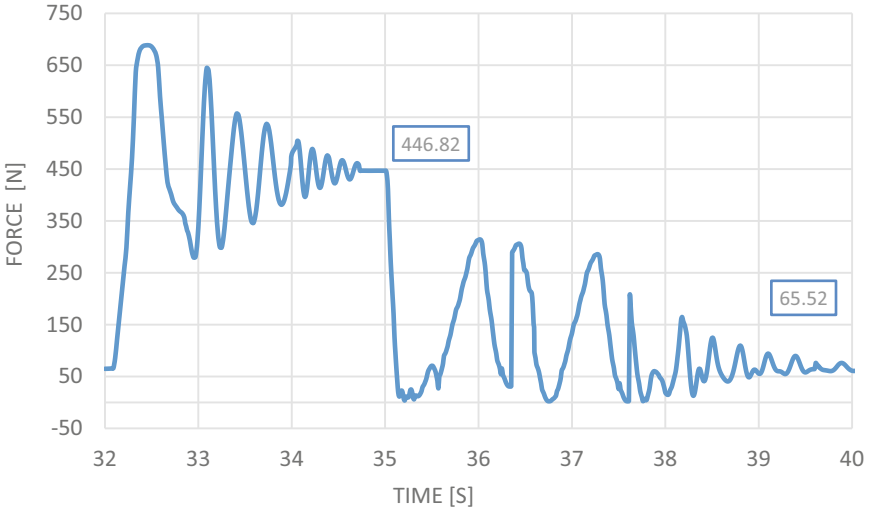

Fig. 7. Time history of force reaction in the experiment; the 7 point loads are added at $t = 32$ s, and they are removed at $t = 35$ s

the force oscillates after load removal, and it does not reach this value again during the vibration that decays. Finally, the force reaches the value of 67.3 N in the static equilibrium of the unloaded cable. The force reaction in the static equilibrium of the loaded cable for the load cases considered is summarized in Table 4 together with the force reaction in the static equilibrium of the unloaded cable, which is reached after load shedding in each case. The coincidence of the calculated and measured force values as shown by the small discrepancies in the last row confirms the reliability of the model.

Table 4. Force reaction in the static equilibrium before and after load removal

Number of applied point loads	0	3	7	11	17
Experimental tests (N)	65.5	277	447	459	660
Numerical simulations (N)	64.4	266	446	496	653
Discrepancy (%)	–1.68	–3.97	–0.22	8.06	–1.06

5 Conclusion

The research presented in this paper focuses on the study of cable vibration following load removal from different parts of the cable. Numerical simulations and experimental tests were carried out to predict the jump height and the variation of force in the cable during the vibration. These tests model the phenomenon of partial ice shedding from transmission line conductors. Numerical simulations show that the approximation of distributed load with several point loads provides similar jump height and cable tension, and they closely follow the tendencies obtained in the experiments. The jump height increases with increasing the loaded and shedding part in the middle of the span, and a particularly sharp increase is observed in the jump height when the loaded part became more than the half of the span. The force acting at the suspension in the experiments was also closely predicted by the numerical model. Load removal is followed by a decaying oscillation of the force, but its maximum value did not reach the force acting in the static equilibrium of the loaded span.

The dynamic behavior following partial shedding could be better understood after further experiments and numerical simulations when partial load shedding occurs on a fully loaded span. Furthermore, both of the experimental set-up and numerical model are applicable to simulate vibration of a two-span section, which is also part of future research. Experiments with recording the variation of vertical displacement in time during the vibration are recommended for future study. Finally, the validated numerical approach would be applied to simulate load shedding on the model of a full-scale transmission line. Such simulations would reveal the tendencies how the rate and location of ice shedding on the conductor influence the conductor rebound height and the conductor tension during vibration.

Acknowledgements. Project no. TKP2021-NVA-29 has been implemented with the support provided by the Ministry of Culture and Innovation of Hungary from the National Research, Development and Innovation Fund, financed under the TKP2021-NVA funding scheme.

References

1. Morgan, V.T., Swift, D.A.: Jump height of overhead-line conductors after the sudden release of ice loads. Proc. IEE **111**(10), 1736–1746 (1964)
2. Jamaleddine, A., McClure, G., Rousselet, J., Beauchemin, R.: Simulation of ice shedding on electrical transmission lines using ADINA. Comput. Struct. **47**(4/5), 523–536 (1993)
3. Kollár, L.E., Farzaneh, M.: Modeling sudden ice shedding from conductor bundles. IEEE Trans. Power Deliv. **28**(2), 604–611 (2013)
4. Kollár, L.E., Farzaneh, M., Van Dyke, P.: Modeling ice shedding propagation on transmission lines with or without interphase spacers. IEEE Trans. Power Deliv. **28**(1), 261–267 (2013)
5. Yan, B., Chen, K., Guo, Y., Liang, M., Yuan, Q.: Numerical simulation study on jump height of iced transmission lines after ice shedding. IEEE Trans. Power Deliv. **28**(1), 216–225 (2013)
6. Wu, C., Yan, B., Zhang, L., Zhang, B., Li, Q.: A method to calculate jump height of iced transmission lines after ice-shedding. Cold Reg. Sci. Technol. **125**, 40–47 (2016)
7. Huang, G., Yan, B., Wen, N., Wu, C., Li, Q.: Study on jump height of transmission lines after ice-shedding by reduced scale modeling test. Cold. Reg. Sci. Technol. **165** (2019)

8. Kollár, L.E.: Ice-shedding-induced vibration of conductors with active vibration control. Cold. Reg. Sci. Technol. **196** (2022)
9. Lajber, K., Borbély, T., Kollár, L.E., Szilvágyi, M.: Tesztberendezés távvezetékről leszakadó jég keltette lengések modellezésére (in Hungarian). Mérnöki és Informatikai Megoldások/Engineering and IT Solutions **2021**(1), 55–61 (2021)
10. Ammar, M.: Vibration of transmission lines following load shedding, BSc thesis, Savaria Institute of Technology, ELTE Eötvös Loránd University, Budapest, Hungary (2022)